Electronic Supporting Information

Chiral Recognition *Via* a Stereodynamic Vanadium Probe Using the Electronic Circular Dichroism Effect in Differential Raman Scattering

Ewa Machalska, †[a,b] Natalia Hachlica, †[a,b] Grzegorz Zajac,[b,c] Davide Carraro,[d] Malgorzata Baranska,[a,b] Giulia Licini,[d] Petr Bouř,*[c] Cristiano Zonta*[d] and Agnieszka Kaczor*[a,b]

[a] Faculty of Chemistry, Jagiellonian University, Gronostajowa 2, Krakow 30-387, Poland

[b] Jagiellonian Centre for Experimental Therapeutics (JCET), Jagiellonian University, Bobrzynskiego 14,
Krakow 30-348, Poland

[c] Institute of Organic Chemistry and Biochemistry, Academy of Sciences, Flemingovo náměstí 2, 16610, Prague, Czech Republic

[d] Dipartimento di Scienze Chimiche, Università degli Studi di Padova and CIRCC, Padova Unit, 35131 Padova, Italy

† these authors contributed equally

* corresponding authors

Content

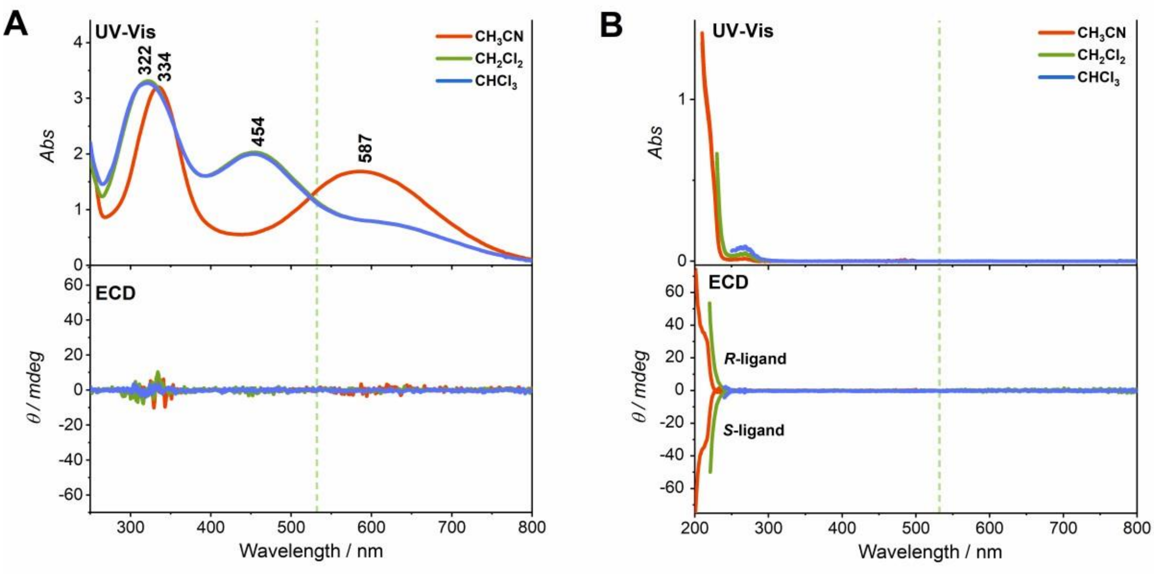

Fig. S1. UV-vis and ECD spectra of oxo-vanadium(V) aminotriphenolate (**panel A**) as well as *S*- and *R*- enantiomers of *N*-(1-phenylethyl)acetamide (**panel B**) measured in $CHCl_3$, CH_2Cl_2 and CH_3CN. The green dotted lines indicate the excitation wavelength of the ROA laser (532 nm).

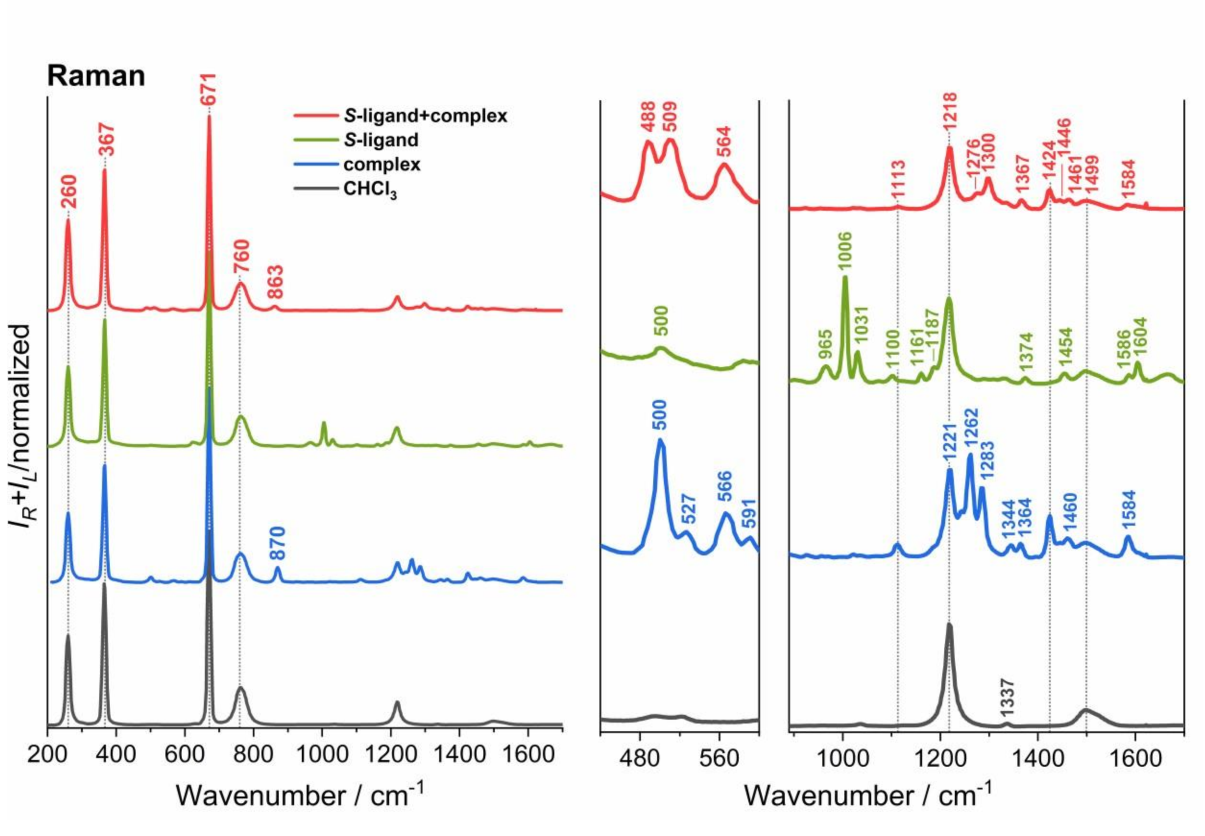

Fig. S2. Comparison of normalized Raman spectra of the mixture (***S*-ligand+complex**) of oxo-vanadium(V) aminotriphenolate ($1{\cdot}10^{-4}$ mol·dm^{-3}) in presence of *S*-stereoisomer of *N*-(1-phenylethyl)acetamide ($8{\cdot}10^{-4}$ mol·dm^{-3}) in $CHCl_3$ as well as pure *S*-stereoisomer of *N*-(1-phenylethyl)acetamide (***S*-ligand**, $3{\cdot}10^{-1}$ mol·dm^{-3}) and pure oxo-vanadium(V) aminotriphenolate (**complex**, $3{\cdot}10^{-5}$ mol·dm^{-3}) in $CHCl_3$.

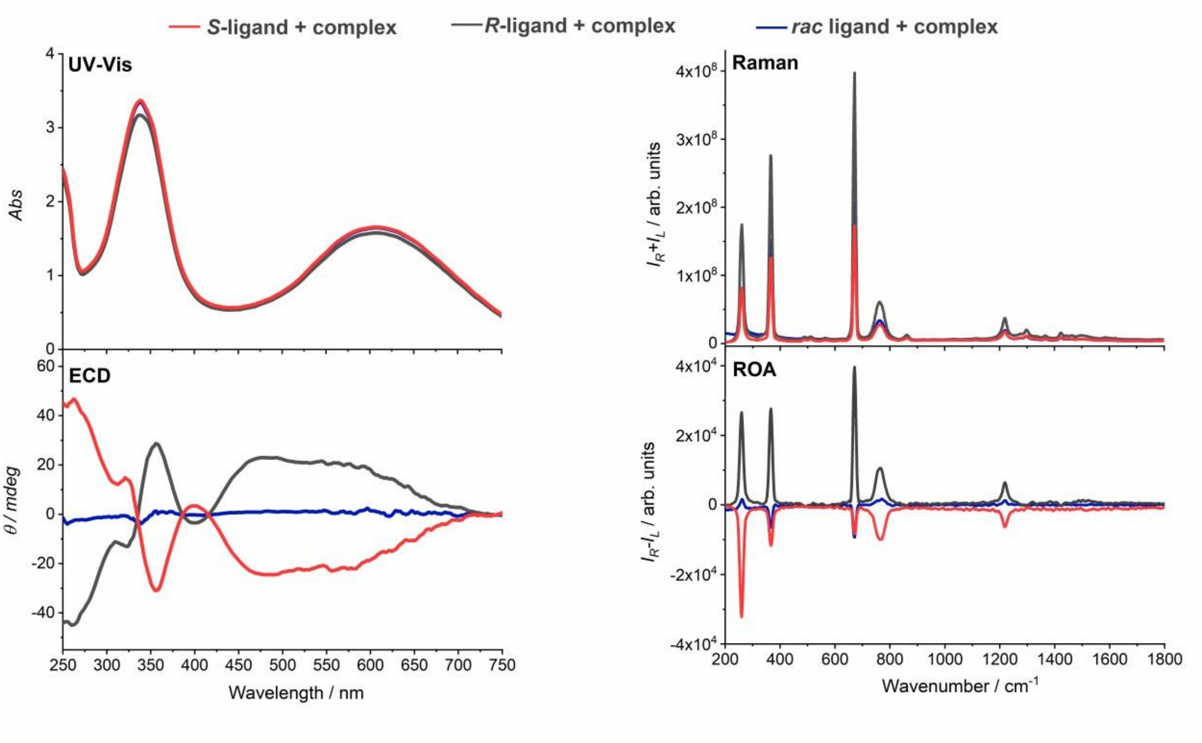

Fig. S3. UV-vis, ECD, Raman and ROA spectra of the supramolecule composed of oxo-vanadium(V) aminotriphenolate and the racemic mixture of *S*- and *R*- enantiomers of *N*-(1-phenylethyl)acetamide in $CHCl_3$. Ligand and complex concentrations are $8{\cdot}10^{-4}$ mol·dm^{-3} and $1{\cdot}10^{-4}$ mol·dm^{-3} respectively. ROA spectra have dominant contribution from ECD-Raman.

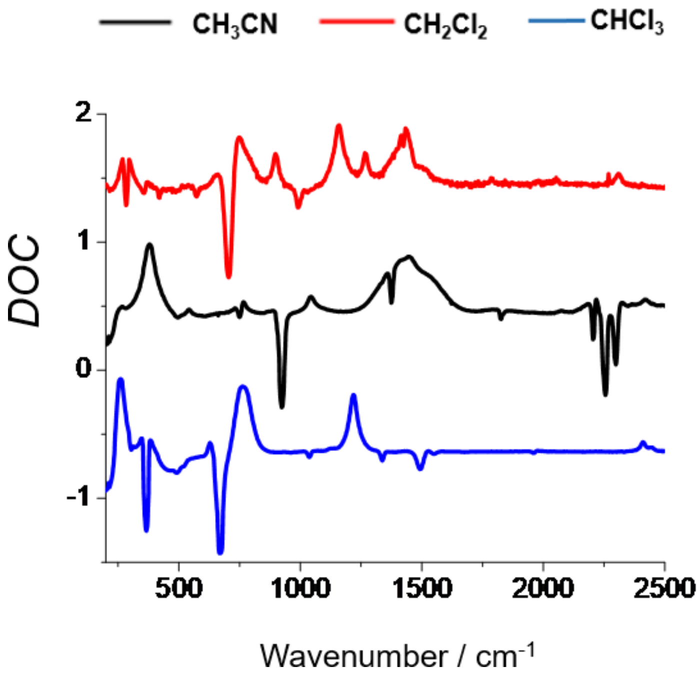

Fig. S4. Experimental DOC(R) spectra for $CHCl_3$, CH_2Cl_2, and CH_3CN.

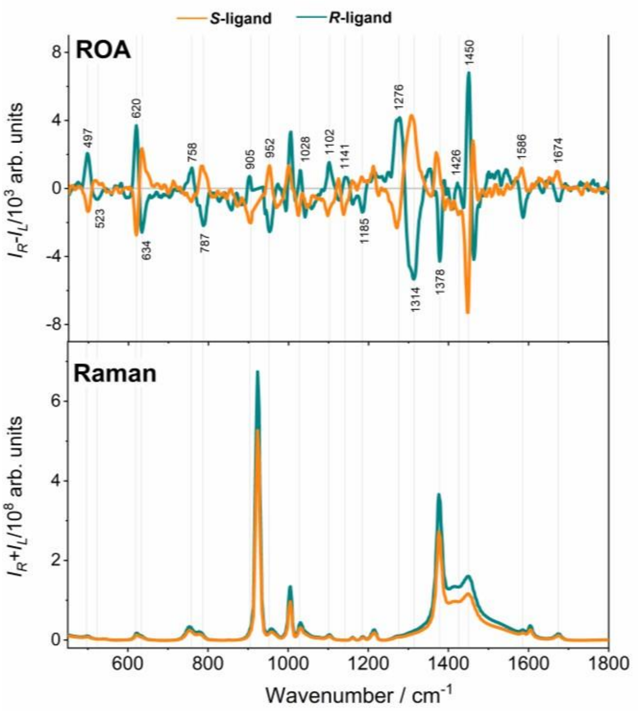

Fig. S5. Raman and ROA spectra of pure *N*-(1-phenylethyl)acetamide in CH_3CN ($3.2\cdot10^{-1}$ mol·dm^{-3}).

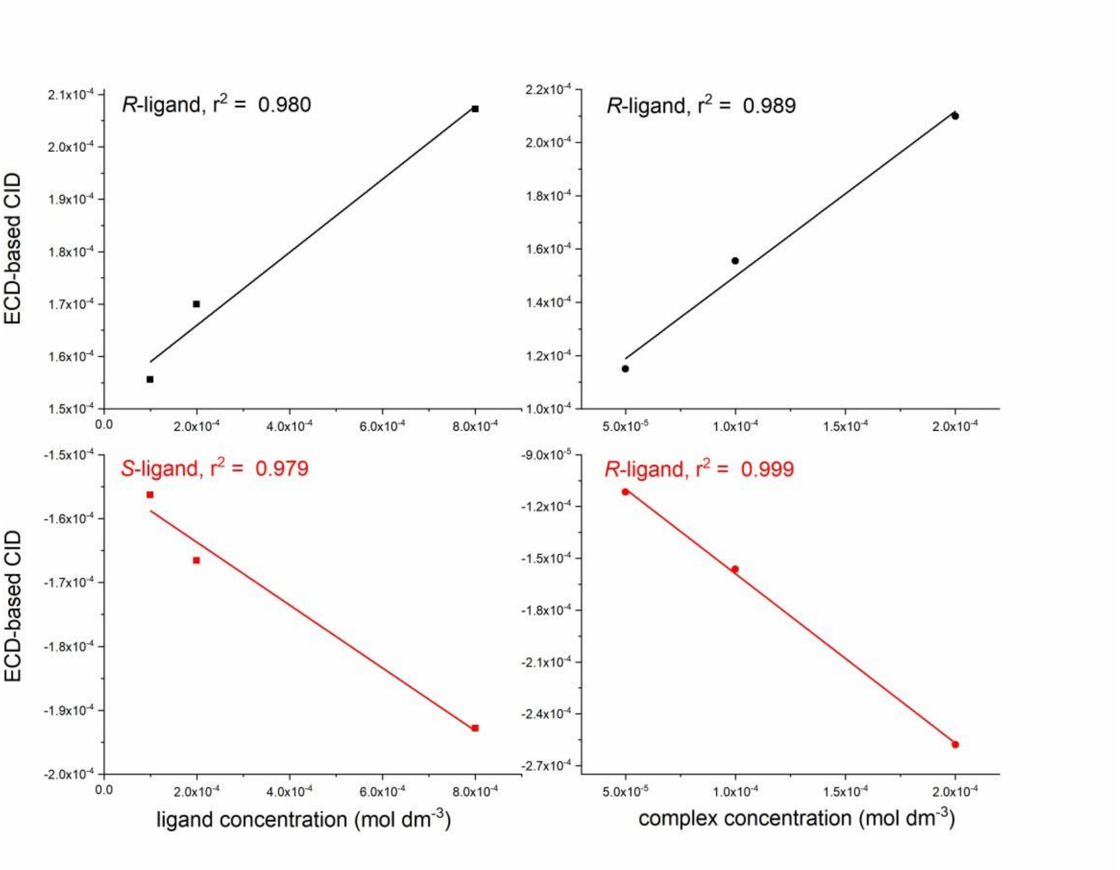

Fig. S6. CID dependence on ligand and complex concentrations for the band at 760 cm^{-1}. For varied ligand concentrations, complex concentration was constant and equal to $1\cdot10^{-4}$ mol·dm^{-3} and vice versa.

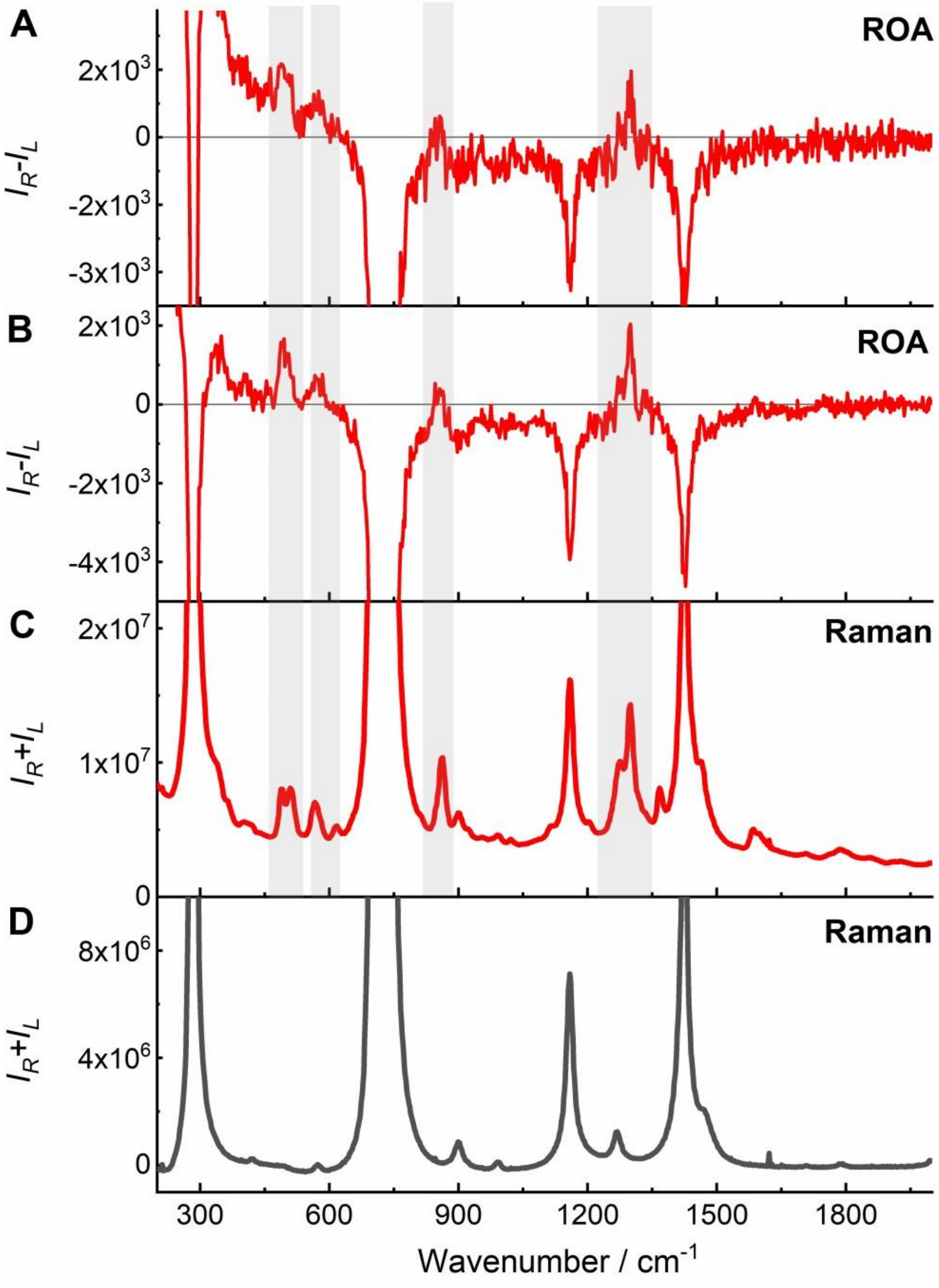

Fig. S7. ROA (12 and 48 hours accumulation time in **A** and **B**, respectively) and Raman (**C**) spectra of the unit composed of oxo-vanadium(V) aminotriphenolate ($1\cdot10^{-4}$ mol·dm^{-3}) and *S*-enantiomer of *N*-(1-phenylethyl)acetamide ($8\cdot10^{-4}$ mol·dm^{-3}) in CH_2Cl_2 showing low-intensity signals due to the complex (denoted grey, 300 mW). Raman spectrum of a pure CH_2Cl_2 given as a black line (**D**). ROA spectra have dominant contribution from ECD-Raman of the solvent.

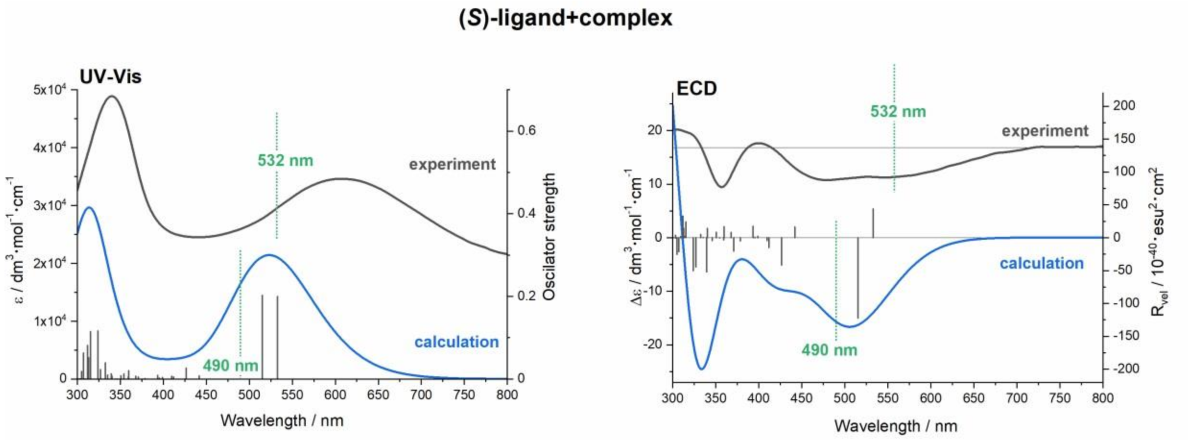

Fig. S8. Comparison of experimental and DFT calculated UV-Vis and ECD spectra of the supramolecule composed of oxo-vanadium(V) aminotriphenolate and *S* enantiomer of *N*-(1-phenylethyl)acetamide in CH_2Cl_2. Ligand and complex concentrations are $8{\cdot}10^{-4}$ mol·dm^{-3} and $1{\cdot}10^{-4}$ mol·dm^{-3}, respectively. Black lines are theoretical oscillator and rotatory strengths; green dotted lines show experimental and theoretical ROA/Raman incident light wavelength.

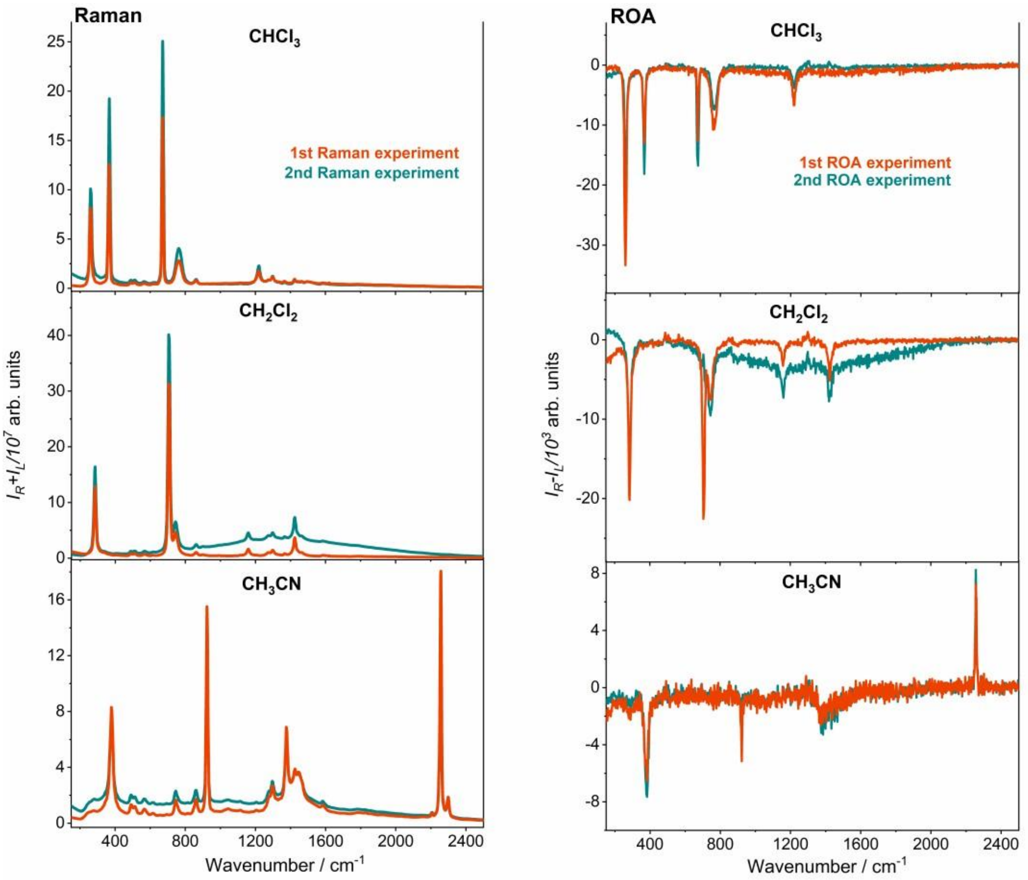

Fig. S9. Raman and ROA (mainly ECD-Raman) spectra of the unit built from oxo-vanadium(V) aminotriphenolate and as *S* stereoisomer of *N*-(1-phenylethyl)acetamide measured in $CHCl_3$, CH_2Cl_2 or CH_3CN, respectively, obtained based on two independent measurements of two independent samples. Presented spectra were averaged for 24 ($CHCl_3$, CH_2Cl_2) or 12 (CH_3CN) hours.

Table S1. Comparison of CID values calculated based on experimental Raman and ROA spectra and experimental DOC and ECD spectra of the supramolecular system composed of oxo-vanadium(V) aminotriphenolate (complex), *N*-(1-phenylethyl)acetamide (ligand) and $CHCl_3$ for depolarized bands.

Complex concentration (mol·dm^{-3})	**Ligand concentration (mol·dm^{-3})**	**Band wavenumber (cm^{-1})**	**CID[a] for *R* stereoisomer**		**CID[a] for *S* stereoisomer**	
			ROA/Raman intensity	$\frac{\theta_s' + DOC \cdot \theta_s}{131\,952}$	**ROA/Raman intensity**	$\frac{\theta_s' + DOC \cdot \theta_s}{131\,952}$
$5\cdot10^{-5}$	$1\cdot10^{-4}$	260	$1.7\cdot10^{-4}$	$1.3\cdot10^{-4}$	$-1.3\cdot10^{-4}$	$-1.4\cdot10^{-4}$
		760	$1.5\cdot10^{-4}$	$1.2\cdot10^{-4}$	$-1.2\cdot10^{-4}$	$-1.1\cdot10^{-4}$
		1218	$9.5\cdot10^{-5}$	$1.0\cdot10^{-4}$	$-9.4\cdot10^{-5}$	$-1.2\cdot10^{-4}$
$1\cdot10^{-4}$	$1\cdot10^{-4}$	260	$1.1\cdot10^{-4}$	$1.9\cdot10^{-4}$	$-1.4\cdot10^{-4}$	$-1.7\cdot10^{-4}$
		760	$1.3\cdot10^{-4}$	$1.6\cdot10^{-4}$	$-1.2\cdot10^{-4}$	$-1.6\cdot10^{-4}$
		1218	$1.9\cdot10^{-4}$	$1.6\cdot10^{-4}$	$-1.1\cdot10^{-4}$	$-1.7\cdot10^{-4}$
$1\cdot10^{-4}$	$2\cdot10^{-4}$	260	$2.1\cdot10^{-4}$	$1.5\cdot10^{-4}$	$-1.1\cdot10^{-4}$	$-1.5\cdot10^{-4}$
		760	$2.3\cdot10^{-4}$	$1.7\cdot10^{-4}$	$-1.1\cdot10^{-4}$	$-1.7\cdot10^{-4}$
		1218	$2.3\cdot10^{-4}$	$1.4\cdot10^{-4}$	$-1.2\cdot10^{-4}$	$-1.7\cdot10^{-4}$
$1\cdot10^{-4}$	$8\cdot10^{-4}$	260	$1.5\cdot10^{-4}$	$2.0\cdot10^{-4}$	$-3.9\cdot10^{-4}$	$-2.1\cdot10^{-4}$
		760	$1.6\cdot10^{-4}$	$2.1\cdot10^{-4}$	$-3.6\cdot10^{-4}$	$-1.9\cdot10^{-4}$
		1218	$1.9\cdot10^{-4}$	$1.8\cdot10^{-4}$	$-4.3\cdot10^{-4}$	$-1.8\cdot10^{-4}$
$2\cdot10^{-4}$	$1\cdot10^{-4}$	260	$2.4\cdot10^{-4}$	$2.3\cdot10^{-4}$	$-2.2\cdot10^{-4}$	$-2.8\cdot10^{-4}$
		760	$2.5\cdot10^{-4}$	$2.1\cdot10^{-4}$	$-2.1\cdot10^{-4}$	$-2.6\cdot10^{-4}$
		1218	$2.4\cdot10^{-4}$	$2.1\cdot10^{-4}$	$-1.3\cdot10^{-4}$	$-1.7\cdot10^{-4}$

[a] ECD signal expressed as ellipticity (in m°), assumed 1 cm ROA pathlength.